

https://doi.org/10.1070/QEL16692

Nano- and femtosecond high-repetition-rate multipulse laser irradiation of dehydrated bone tissue: role of accumulated heat and model of cooling

A.V. Belikov, A.A. Shamova, G.D. Shandybina, E.B. Yakovlev

Abstract. **A model is proposed to describe the cooling of a biotissue surface after irradiation by a series of laser pulses. The spatial distribution of heat accumulated by the surface of a hard biotissue irradiated by nano- and femtosecond laser pulses is qualitatively estimated as a function of the pulse repetition rate. The obtained results are compared with the data of experimental irradiation of dry bone with both nanosecond and femtosecond laser pulses. The key contribution of the variation of the biotissue optical characteristics to the dependence of heat, accumulated by its surface, on the repetition rate of nanosecond laser pulses is demonstrated. The mechanism of the pulse repetition rate affecting the residual heat in the biotissue is more complex and requires adequate consideration of the change in its optical and thermophysical parameters. The application of the cooling model allowed substantial confirmation of the key role of the accumulated heat in the process of hard tissue carbonisation around the area of laser impact and the necessity of external cooling in the course of high-repetition-rate multipulse laser processing using both nanosecond and femtosecond pulses.**

Keywords: *nanosecond and femtosecond laser pulses, hard biological tissues, carbonisation, accumulated heat.*

1. Introduction

At present, laser radiation is extensively used in medicine, including stomatology and orthopaedics [1–4]. During recent decades, the possibility of using different lasers that operate both in UV and in IR spectral ranges for processing hard tissues has been investigated [5–7]. The most efficient laser ablation of tooth and bone tissues was achieved using Er:YAG ($\lambda = 2.94$ μm) and CO_2 ($\lambda = 10.6$ μm) lasers [8–13]. This is because their radiation wavelengths correspond to the fundamental absorption peaks of hard tissues.

Recent research and development allowed the development of compact, high-efficiency and economical ytterbium fibre lasers with an oscillation wavelength of 1.070 μm. Strong scattering and weak absorption of their radiation [4, 14] limits the application of these lasers to the processing of hard tissues. At the same time, the ytterbium fibre laser has certain advantages in surgery of hard tissues as compared to the solid-state Er:YAG laser and gas CO_2 laser. The fibre radiation delivery system of the ytterbium laser provides irradiation of tissue regions difficult to access, and the high output pulse power and repetition rate allows a high rate of ablation [14].

It is also rather promising to study possible application of femtosecond lasers to the processing of bone tissue [15–17]. In contrast to the Er:YAG laser pulses, the effect of femtosecond laser pulses on a biotissue practically does not influence the relative content of phosphorus and calcium in the tissue, which facilitates the postoperative healing of the bone [18].

Due to the high sensitivity of biotissues to thermal damage, an urgent problem is to optimise the parameters of lasers in order to provide safe and precise surgical operation. The rate of laser processing should be comparable with that using mechanical means or exceed it, which requires the employment of the regimes of high-repetition-rate multipulse irradiation.

The analysis shows that for these purposes lasers emitting short [19–21] and ultrashort [22–25] pulses with rather different pulse repetition rates, from tens of hertz to hundreds of megahertz, are used. The laser processing with ultrashort pulses has a number of advantages over the laser processing with nanosecond pulses, since the duration of the laser pulse is smaller than the time of electron–phonon energy transfer, and all thermal, chemical, and mechanical processes develop after the pulse terminates [26–28]. At the same time, physical and chemical mechanisms of laser heating and ablation of biological media are extremely complex. This is, first, due to the complexity of the object itself, as well as to the considerable difference in the processes of interaction between the laser radiation and the biotissue under the conditions of varying not only the laser pulse duration, but also the radiation wavelength, light flux density, pulse repetition rate, etc. The pulse-periodic irradiation with both short and ultrashort pulses can lead to the residual heating [29] and cause carbonisation (charring) of the hard tissue around the exposed region [30, 31]. Under the high-repetition-rate multipulse laser impact, the contribution of residual heat to the process of biotissue treatment can increase with increasing pulse repetition rate, leading to the consequences that include negative ones. In this connection, it is necessary to analyse and compare the specific features of thermal impact of trains of high-repetition-rate laser pulses on biological tissues under pulse-periodic irradiation.

The analysis of spatiotemporal distribution of temperature in the irradiated region requires the application of labour-consuming methods of numerical modelling [7]. However, at the initial stage of studies the simplified estimates of thermal processes, which do not contradict experimental data, can help in revealing the factors that above all affect the result of laser processing.

A.V. Belikov, A.A. Shamova, G.D. Shandybina, E.B. Yakovlev ITMO University, Kronverkskii prosp. 49, 197101 St. Petersburg, Russia; e-mail; corchand@gmail.com

Received 31 March 2018; revision received 21 May 2018
Kvantovaya Elektronika **48** (8) 755–760 (2018)
Translated by V.L. Derbov

The aim of the present paper is to qualitatively estimate the spatial distribution of accumulated heat on the surface of a hard biotissue irradiated by nanosecond and femtosecond laser pulses as a function of their repetition rate and to reveal the major factors that determine the process of residual heating and cause carbonisation. The obtained results are compared with those of the experimental studies on the irradiation of dry skin by nanosecond laser pulses carried out by the authors, as well as the experimental data on femtosecond laser processing, presented in Ref. [32].

2. Theoretical modelling: the model of cooling

Since the bone tissue has a complex structure, multicomponent composition, and high water content, the interaction of laser radiation with bone is significantly complicated due to a variety of initiated physical and chemical processes (e.g., water boiling, carbonisation, evaporation of organic substances, etc.) that take place in this biological tissue at different temperatures [7]. In this connection, to simplify the analysis of thermal processes aimed at revealing the main factors that determine the accumulated heating under the impact of nanosecond and femtosecond laser radiation on the hard biotissue, we considered the dehydrated (dry) bone as an object of study for constructing the cooling model. It is considered as a quasi-homogeneous medium with averaged values of optical and thermophysical characteristics.

Although the heating process develops during a nanosecond pulse or after the end of a femtosecond one, the cooling stage is much longer in both cases [33]. This stage determines the process of thermal afteraction in the case of pulse-periodic laser processing both in the femtosecond range and in the nanosecond one.

At low thermal conductivity typical of biological tissues the thickness of the region heated due to heat conductivity for short and ultrashort pulses is usually much smaller than the irradiation zone size. Therefore, one can assume that the distribution of temperature in the impact zone at the initial moment of cooling repeats the distribution of the absorbed energy density, i.e., the Gaussian transverse distribution, which is conserved at any depth and exponentially decreases with z (the z axis is directed deep into the tissue):

$$T(r,z) = T_{\max}\exp(r^2/r_0^2)\exp(-\alpha z), \tag{1}$$

where $T_{\max}$ is the maximal temperature of heating, from which the cooling begins; α is the absorption coefficient of bone tissue; and r_0 is the radius of the laser beam spot.

In laser surgery, one of important indicators of high efficiency of invasion is the maximal incision depth with a minimal thermal damage of surrounding tissues. In this connection the determination of optimal regimes of the bone tissue laser processing makes it necessary to consider the effects that occur not only at the tissue surface, but also in its volume. In the course of interaction of laser radiation with hard biotissue at the wavelength 1.07 μm, apart from the absorption there occurs strong scattering of radiation (in this case the scattering coefficient of bone tissue amounts to ~17 cm^{-1} [34]). Therefore, to change the radiation intensity in the process of propagation through the biotissue, in Eqn (1) one should replace the absorption coefficient α with the extinction coefficient, equal to the sum of the absorption and scattering coefficients [35]. In this case the problem becomes essentially complicated, since the necessity of additional studies of the dependence of the scattering coefficient on the irradiation regime parameters arises, which is beyond the scope of the present paper. Therefore, we restrict ourselves to considering thermal processes at the bone surface.

Assuming that all absorbed energy is used to heat the medium, we can express the maximal temperature of the surface heating as

$$T_{\max} = \alpha AE/C, \tag{2}$$

where A and C are the absorptivity and heat capacity of the bone tissue, respectively.

The cooling of the heated region is described by the equation

$$\frac{\partial T}{\partial t} = a\frac{\partial^2 T}{\partial r^2} + \frac{1}{r}\frac{\partial T}{\partial r} \tag{3}$$

(a is the thermal diffusivity of bone tissue) with an initial temperature distribution

$$T(r,0) = T_{\max}\exp(r^2/r_0^2). \tag{4}$$

Applying the direct Hankel transform of the zeroth order [36]

$$\frac{\partial \bar{T}}{\partial t} = a\lambda^2\bar{T}(\lambda,t),$$

where

$$\bar{T}(\lambda,0) = \frac{T_{\max}r_0^2}{2}\exp\left(-\frac{\lambda^2 r_0^2}{4}\right),$$

and then the inverse Hankel transform, we arrive at the temperature distribution in coordinate and time after the end of the first pulse:

$$T(t,r) = \frac{T_{\max}r_0^2}{r_0^2 + 4at}\exp\left(-\frac{r^2}{r_0^2 + 4at}\right). \tag{5}$$

The accumulated temperature, i.e., the temperature of the biotissue surface at a distance r from the axis of the laser beam without the initial (room) temperature taken into account, after the impact of N pulses with the repetition rate f at the time of arrival of the N + 1th pulse will amount to

$$T\left(t = \frac{N}{f}, r\right) = T_{\max}\sum_{i=1}^{N}\frac{r_0^2}{r_0^2 + 4ail/f}\exp\left(-\frac{r^2}{r_0^2 + 4ail/f}\right). \tag{6}$$

3. Experimental study of high-repetition-rate multipulse irradiation of dehydrated bone tissue by nanosecond laser pulses: role of accumulated heat and application of the cooling model

In the experiment, we used a MiniMarker 2.0 setup (OOO 'Lazernyi Tsentr', Russia) based on an ytterbium pulsed fibre laser with a mean radiation power P_{av} of up to 20 kW, equipped with a translation stage and a Gentec-EO SOLO2 microprocessor energy meter (Gentec Electro-Optics, Inc., Canada). We also used an Axio Imager.Aim microscope (Carl Zeiss, Germany) with a CCD camera for orthoscopic and conoscopic observations. The sample was a deer bone,

preliminary dried at room temperature during 6 months after extraction and having the thickness 4 ± 0.2 mm. The sample was irradiated in the focal plane of the long-focus objective with a beam spot radius in the waist region 30 ± 3 μm during 10 seconds with varied pulse repetition rate.

At the first stage the sample was irradiated at different points with different mean power of radiation, varying the pulse power P_p from the maximal value and the pulse repetition rate f (Fig. 1, points 1–7). For the regimes of irradiation used at points 1–3 we observed the straight-through destruction of the bone, at point 4 the destruction was present, and at points 5–7 the bone was not damaged. Points 8–14 were irradiated with the energy density $E = 3.5$ J cm^{-2} (the error smaller than 10%) and the pulse repetition rate varying from 35 to 5 kHz with a step of 5 kHz (Fig. 1).

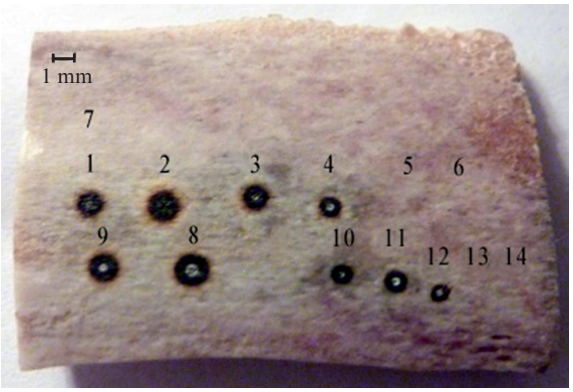

Figure 1. Photograph of dry bone after irradiation: points 1 and 2 are shown for the mean power $P_{av} = 16$ W, the pulse power $P_p = 6.6$ kW, the energy density $E = 11.6$ J cm^{-2}, the pulse repetition rate $f = 50$ kHz; point 3 – $P_{av} = 6$ W, $P_p = 4$ kW, $E = 10.6$ J cm^{-2}, $f = 30$ kHz; point 4 – $P_{av} = 2.7$ W, $P_p = 2.7$ kW, $E = 4.8$ J cm^{-2}, $f = 20$ kHz; point 5 – $P_{av} = 1$ W, $P_p = 2$ kW, $E = 3.5$ J cm^{-2}, $f = 10$ kHz; point 6 – $P_{av} = 0.7$ W, $P_p = 1.4$ kW, $E = 2.5$ J cm^{-2}, $f = 10$ kHz; point 7 – $P_{av} = 0.4$ W, $P_p = 1.4$ kW, $E = 2.5$ J cm^{-2}, $f = 5$ kHz; points 8–14 – $P_{av} = 3.5$–0.5 W, $P_p = 2$ kW, $E = 3.5$ J cm^{-2}, $f = 35$–5 kHz with a step of 5 kHz, respectively. The laser radiation wavelength is 1.070 μm, and the exposure time is 10 s.

Figure 2 presents the dependence of the outer diameter of the damaged region (carbonisation zone) on the pulse repetition rate from points 8–14 of Fig. 1. It is seen that at $f <$ 15 kHz the bone surface is not damaged. At $f \sim 15$ kHz the damage appears in the form of darkening, and then the size of the damaged region increases with increasing repetition rate. As shown by our analysis of the bone tissue surface by means of the optical microscope, the damaged region consists of the outer dark wide ring of carbonised bone, the light narrow ring of metamorphised bone, and the small central zone of ablation.

The repetition rate dependence of the damaged bone outer diameter observed in the experiment at $E = 3.5$ J cm^{-2} is an evidence of essential influence of the pulse repetition rate on the size of laser damage of dry bone. A remarkable fact is a sharp increase in the outer diameter of the carbonisation zone at $f > 10$ kHz. The nature of this effect remains unclear. To clarify it at the presented regimes of laser processing of dry bone, we performed qualitative estimations of heat accumulation according to the cooling model. In the modelling, we used the values of parameters of the laser radiation and the bone tissue, averaged over the literature sources [7, 32, 37].

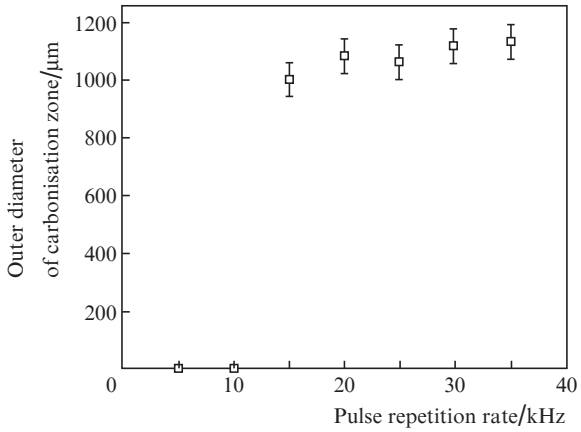

Figure 2. Experimental dependence of the outer diameter of the carbonisation zone of dry bone (points 8–14) on the repetition rate of laser pulses at the radiation wavelength 1.070 μm, the pulse duration 50 ns, the mean power 2 kW, the energy density 3.5 J cm^{-2}, and the exposure time 10 s.

Energy density of laser pulse E/J cm^{-2}	3.5
Laser pulse duration τ/ns	50
Beam spot radius of laser radiation (at the level e^{-2}) r_0/μm	30
Exposure time t/s	10
Pulse repetition rate f/kHz	1–40
Bone tissue absorptivity A	0.22–1 [32]
Bone tissue absorption coefficient α/cm^{-1}	10–25 [7]
Bone tissue heat conductivity k/W cm^{-1} K^{-1}	3.56×10^{-2} [37]
Bone tissue heat capacity C/J cm^{-3} K^{-1}	1.4 [32]
Bone tissue thermal conductivity α/cm^2 s^{-1}	2.5×10^{-2}

The radial distributions of the accumulated temperature of the dry bone surface irradiated during 10 s with the nanosecond laser pulses having the repetition rate 1, 10, and 15 kHz calculated according to Eqn (6) are presented in Fig. 3. Curves (*1*–*3*) are calculated for the constant absorption coefficient $\alpha = 10$ cm^{-1} and absorptivity $A = 0.22$. One can see that for the repetition rate 1 kHz the residual heating does not exceed 30 °C and slowly decreases with distance from the irradiation region. For the repetition rates 10 and 15 kHz, the accumulated temperature of the surface exceeds 30 °C and abruptly falls (by nearly 40%) at distances 0.1–0.2 mm from the centre of the irradiation region, and then smoothly decreases at distances 0.2–0.6 mm.

From the comparison of the theoretical radial temperature distribution presented in Fig. 3a with the images of the bone tissue areas experimentally irradiated by nanosecond pulses (Fig. 1) one can notice that the accumulated temperature of the bone tissue surface obtained in the calculations for any of the three pulse repetition rates does not exceed 56.7 °C. At the same time, in the experiment (Fig. 1) for the repetition rates 1 and 10 kHz the surface of the bone tissue is not changed by the laser impact, which is generally typical for small values of the accumulated (residual) temperature. At the repetition rate 15 kHz the ablation crater is formed, surrounded by the zones with metamorphised and carbonised tissue, which is possible only at temperatures significantly exceeding those obtained in the calculations for the constant optical characteristics α and A [7, 38–46].

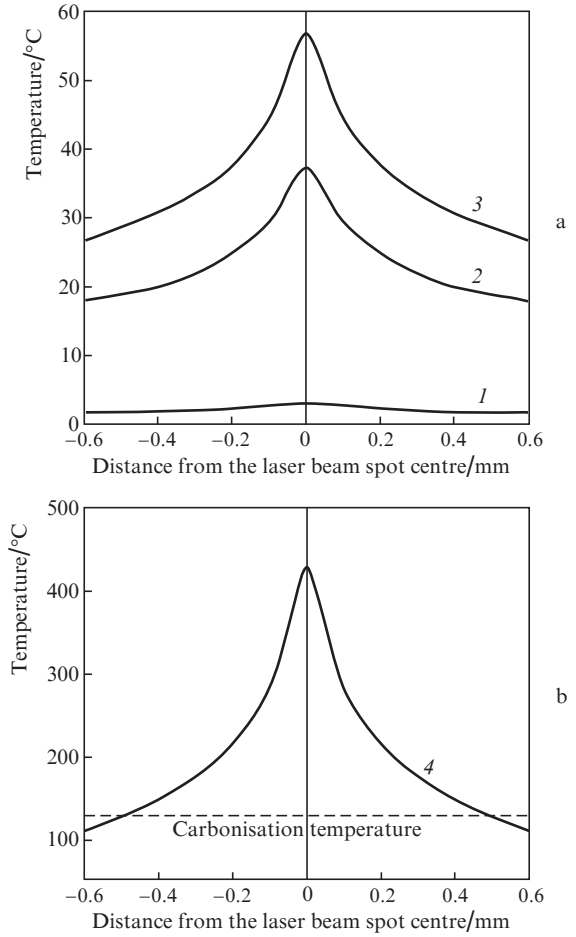

Figure 3. Theoretical radial distribution of temperature, accumulated by the dry bone tissue surface, in the region surrounding the area of laser action under the high-repetition-rate multipulse nanosecond irradiation: (a) at constant α and A for f = (*1*) 1, (*2*) 10, and (*3*) 15 kHz and (b) at variable α and A for f = 15 kHz.

This discrepancy can be eliminated, if we allow for a change in optical characteristics (α and A) due to blackening of the irradiated zone in expression (6). It is known that a temperature rise facilitates the development of carbonisation of hard biotissue. The carbonisation is a process, in which the hydrogen is released from the organic molecules with the formation of finely dispersed carbon (soot). The process is implemented at definite temperatures and has a nidal character [7]. We should note that in different papers the carbonisation temperatures have significantly different values, namely, above 100 °C [38], 150 °C [37, 39–42], 200 °C [43, 44], 300 °C [7, 45]. This is due to, first, the effect of the exposure time on the result of laser action and, second, the specificity of particular biotissue. The highest temperatures of carbonisation were reported for the biotissues, initially containing water [46]. It is known [7] that already at 60 °C an irreversible damage of biotissue occurs, its colour becomes greyish, and under further heating to the temperature of about 80 °C the collagen fibres starts denaturating. In the case of irradiating a dry biotissue, the energy is not used for water removal from the tissue pores, which can reduce the energy required to achieve the carbonisation temperature. In this connection, it is quite probable that the carbonisation of dry bone can begin at a temperature of ~150 °C. In our case the temperature of carbonisation in Fig. 3b is presented without considering the room temperature (20 °C), i.e., ~130 °C. The carbonised frame exists at temperatures up to 400–500 °C [7] and is burned away with further temperature growth.

In the experiment, at the repetition rate 15 kHz the dependence of the outer diameter of the carbonisation zone of dry bone on the exposure time was determined. In Fig. 4, it is seen that the surface damage (carbonisation) occurs at the sixth second of irradiation. In this connection, in Eqn (6) used to calculate the accumulated temperature of the surface at the repetition rate f = 15 kHz we replaced the initial values α = 10 cm^{-1} and A = 0.22 with α = 15 cm^{-1} and A = 1 at the time from the 6th to the 10th second of irradiation [curve (*4*) in Fig. 3b]. According to the performed calculation, the temperature of the dry bone tissue surface irradiated by nanosecond pulses with the repetition rate f = 15 kHz exceeds the carbonisation temperature as a result of residual heating and the change in optical characteristics at the distances from the beam spot centre, significantly greater than the size of the laser beam spot and approaching 0.5 mm. This corresponds to the outer diameter of the carbonised region, observed in the experiment at the temperature 20 °C. It is worth noting that the residual heating can be essentially reduced at the expense of external air or water cooling, which will facilitate an increase in pulse repetition rate, at which carbonisation begins. Thus, the external cooling will increase the speed of the bone tissue excision because of increasing the pulse repetition rate without changing individual parameters of the pulses.

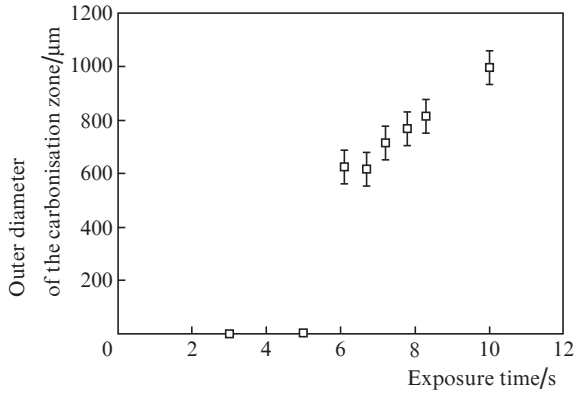

Figure 4. Experimental dependence of the outer diameter of the dry bone carbonisation zone on the exposure time at the laser wavelength 1.070 μm, the pulse duration 50 ns, the pulse repetition rate 15 kHz, the mean power 1.5 W, the pulse power 2 kW, and the energy density 3.5 J cm^{-2}.

4. Theoretical study of high-repetition-rate multipulse irradiation of dehydrated bone tissue by femtosecond laser pulses: comparison with experiment

During a femtosecond laser pulse only the photophysical processes have time to develop, while the thermal, chemical and mechanical processes manifest themselves after the pulse terminates.

The characteristic time of laser energy transfer into the thermal energy amounts to picoseconds, and the maximal heating temperature, from which the cooling begins, is also

achieved after the end of the pulse [3]. In the case of ultrashort pulses, the stage of cooling is much longer than the stages of photoexcitation and heating together [33]. Therefore, one can consider the possibility of using the cooling model for estimating the residual heating under irradiation with femtosecond laser pulses.

In the modelling we used the optical and thermophysical characteristics of bone tissue, presented in Section 3, and the parameters of laser regimes were taken from Ref. [32], the experimental data of which are compared with the results of calculation obtained within the framework of the cooling model. The radiation from the femtosecond laser (λ = 1030 nm, τ = 320 fs, f = 1 Hz–2 MHz) was focused into a spot with the diameter 12.6 μm. The energy density of the laser pulse amounted to ~40 J cm^{-2}. A dry bovine bone a few millimetres thick was irradiated during 10 s with different pulse repetition rates. By means of a thermal imaging camera the average temperature of the bone surface was measured [32].

Figure 5 presents the radial distribution of accumulated temperature of the dry bone tissue surface under irradiation with femtosecond pulses having the repetition rate 1 kHz during 10 s, calculated according to Eqn (6) and obtained by processing the results of thermal measurements [32]. One can see satisfactory agreement between the theoretical curve and the experimental one.

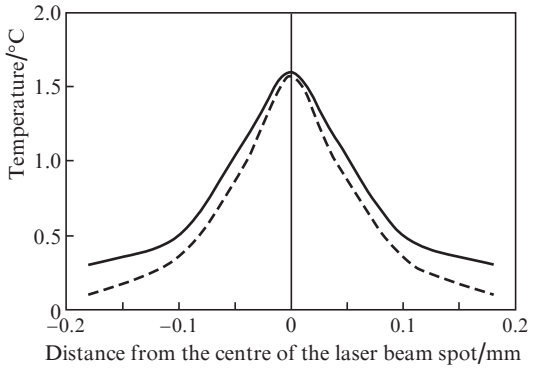

Figure 5. Experimental and theoretical radial distribution of the accumulated temperature of the dry bone tissue surface (relative to the room temperature) in the region surrounding the zone of laser impact under the high-repetition-rate multipulse femtosecond irradiation for f = 1 kHz. The solid curve is the result of calculation (cooling model); the dashed curve is the result of the experiment [32].

In the experiment presented in Ref. [32], the average accumulated temperature of the dry bone tissue surface (relative to the room temperature) under irradiation with different pulse repetition rates was also measured (Fig. 6).

It is seen (the dashed line in Fig. 6) that with an increase in the repetition rate from 1 to 20 kHz the temperature rises linearly from 2 °C to 40 °C. These values demonstrate good fit with the straight line calculated for these laser regimes according to Eqn (6) (the solid line in Fig. 6).

At f = 22 kHz in the experiment [32] an abrupt jump of temperature was observed. If the temperature is calculated using Eqn (6) with a change in optical properties due to carbonisation of bone tissue taken into account, the obtained value falls into the confidence interval, presented in Ref. [32] (Fig. 6). According to the data of Ref. [32], the femtosecond ablation of dry bone occurred at f = 1, 10, and 20 kHz without traces of carbonisation. The ring of carbonised tissue appeared only at f = 22 kHz. The nature of an abrupt increase in the surface temperature of bone tissue at certain pulse repetition rate remains to be an open question. Apparently, it is related to the jump of the residual heat, caused by the change in optical and thermophysical parameters of the biotissue, which, possibly, accompanies the modification of the tissue layer, surrounding the laser crater, because of shock and thermal impact of the dry bone ablation products on the walls of the laser crater. However, this hypothesis requires additional experimental and theoretical studies.

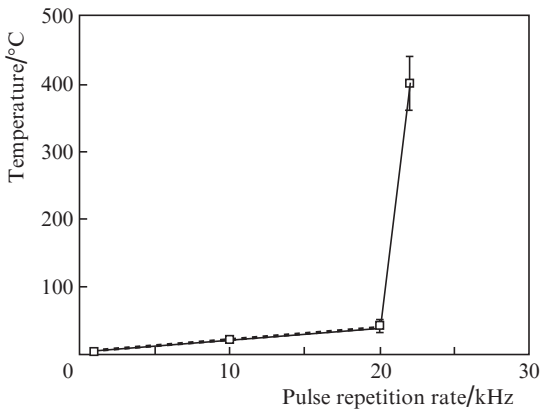

Figure 6. Experimental dependence of the averaged accumulated temperature of the dry bone tissue surface (relative to room temperature) on the repetition rate of femtosecond laser pulses: solid line is the result of calculation (cooling model); dashed line is the result of the experiment [32].

5. Conclusions

The assumption that the cooling stage, being much longer that the heating stage, determines the final result of the thermal afteraction under laser high-repetition-rate multipulse processing of biotissues, allowed a similar approach to apply for the qualitative analysis of the residual heating of dehydrated bone tissue by a series of high-repetition-rate nanosecond and femtosecond laser pulses.

A model of cooling is presented that qualitatively describes the pulse-periodic residual heating for quasi-homogeneous medium with a given initial temperature distribution.

Qualitative estimates of the residual heating of dehydrated bone depending on the repetition rate of nanosecond pulses are compared with the experimentally observed images of its surface damage. The jump of the biotissue surface temperature caused by the growth of the absorption coefficient and absorptivity coincides with the beginning of bone carbonisation.

The comparison of the calculated values of accumulated heat with the experimental results of Ref. [32] devoted to the high-repetition-rate multipulse impact of femtosecond laser pulses on a dry bone has shown the validity of using the model of cooling to estimate the average surface overheating, if the repetition rate is below the values, at which the carbonisation occurs. Additional experimental and theoretical studies are required to explain the appearance of carbonised tissue around the ablation zone and the corresponding jump of the temperature of the bone tissue surface at a certain repetition rate of femtosecond laser pulses.

The qualitative estimates of heat accumulation process under the action of nanosecond and femtosecond laser pulses on the hard tissue, depending on the pulse repetition rate, confirmed the key role of the residual heating in the carbonisation of hard tissue around the impact region. They also proved the necessity of external air or water cooling in the process of high-repetition-rate multipulse laser processing. The application of the cooling model to a particular biological object can essentially simplify the search for optimal parameters of lasers that would provide safety and precision of operations.

Acknowledgements. The work was supported by a grant from the ITMO University (Development of Methods and Devices for Optical and Quantum Informatics Project, Research Work No. 617033).

The authors are grateful to E.V. Kuzmin for preparation of samples and to E.N. Sobol for fruitful discussions.

References

1. Deppe H., Horch H.H. *Lasers Med Sci*., **22**, 217 (2007).
2. Panduric D.G., Bago I., Katanec D., Zabkar J., Miletic I., Anic I. *J. Oral Maxillofac. Surg.*, **70**, 2515 (2012).
3. Sobol E.N., Shekhter A.B., Baskov A.V., in *Lasers for Medical Application: Therapy and Surgery* (Cambridge, UK: Woodhead Publ., 2013) pp 628–658.
4. Sotsuka Y., Nishimoto S., Tsumano T., Kawai K., Ishise H., Kakibuch M., Okihara S.I. *Lasers Med. Sci*., **29**, 1125 (2014).
5. Serafetinides A.A., Makropoulou M.I., Tsikrikas G.N., Helidonis E.S., Kavvalos G., Sobol E.N. *Intern. Soc. Opt. Photon.*, **277**, 62 (1994).
6. Kitai M.S., Sobol E.N., Sviridov A.P., Omel'chenko A.I. *Biophys*., **41**, 1151 (1996) [*Biofiz*., **41**, 1137 (1996)].
7. Sviridov A.P. Dokt. Diss. (M.: IPLIT RAN, 2015).
8. Forrer M., Frenz M., Romano V., Altermatt H.J., Weber H.P., Silenok A., et al. *Appl. Phys. B. Photophys. Las. Chem*., **56**, 104 (1993).
9. Stanislawki M. et al. *Appl. Phys. B. Lasers Opt*., **72**, 115 (2001).
10. Fried N.M., Fried D. *Lasers Surg. Med*., **28**, 335 (2001).
11. Ivanenko M., Fahimi-Weber S., et al. *Lasers Med. Sci*., **17**, 258 (2002).
12. Eyrich G.K. *Med. Laser Appl*., **20**, 25 (2005).
13. Stubinger S., Ghanaati S., et al. *Eur. Surg. Res*., **42**, 150 (2009).
14. Yin C., Ruzzante S.W., Fraser J.M. *Lasers Surg. Med.*, **48**, 288 (2016).
15. Lo D.D., Mackanos M.A., et al. *Lasers Surg. Med*., **44**, 805 (2012).
16. Jeong D.C., Tsai P.S., Kleinfeld D. *Curr. Opin. Neurobiol*., **22**, 24 (2012).
17. Chung S.H., Mazur E. *J. Biophoton.*, **2**, 557 (2009).
18. Ozono K., Obara M. *Appl. Phys. A*, **77**, 303 (2003).
19. Ilgner J.F., Wehner M.M., et al. *J. Biomed. Opt.*, **11**, 014004 (2006).
20. Ivanenko M., Werne M., et al. *Medical Las. Applicat.*, **20**, 13 (2005).
21. Kang H.W., Lee H., et al. *IEEE J. Quantum Electron*., **42**, 633 (2006).
22. Soong H.K., Malta J.B. *Am. J. Ophtalmol*., **157**, 190 (2009).
23. Jeong D.C., Tsai P.S., Kleinfeld D. *Curr. Opin. Neurobiol*., **22**, 24 (2012).
24. Serbin J., Bauer T., Fallnich C., Kasenbacher A., Arnold W.H. *Appl. Surf. Sci.*, **197-198**, 737 (2002).
25. Vogel A., Noack J., et al. *Appl. Phys. B*, **81**, 1015 (2005).
26. Hirayama Y., Obara M.J. *Appl. Phys*., **97**, 064903 (2005).
27. Phipps R. *Laser Ablation and Its Applications* (New York: Springer, 2007).
28. Gamaly E.G., Rode A.V., Luther-Davies B., Tikhonchuk V.T. *Phys. Plasmas*, **9**, 949 (2002).
29. Eaton S.M., Zhang H., Ng M.L., Li J., et al. *Opt. Express*, **16**, 9443 (2008).
30. Miyamoto I., Horn A., et al. *J. Laser Micro/Nanoeng*., **2**, 57 (2007).
31. Marjoribanks R.S., Dille C., Schoenly J.E., McKinney L., Mordovanakis A., Kaifosh P., et al. *Photon. Lasers Med.*, **1**, 155 (2012).
32. Gill R.K., Smith Z.J., Lee C., Wachsmann-Hogiu S. *J. Biophoton.*, **9**, 171 (2016).
33. Veiko V.P., Shakhno E.A., Yakovlev E.B. *Quantum Electron*., **44**, 322 (2014) [*Kvantovaya Elektron*., **44**, 322 (2014)].
34. Bashkatov A.N., Genina E.A., Kochubey V.I., Tuchin V.V. *Proc. SPIE*, **6163**, 616310-7 (2006).
35. Tuchin V.V. (Ed.) *Handbook of Optical Biomedical Diagnostics* (Bellingham, Washington: SPIE Press, 2016) Vol. 2.
36. Gradshtein I.S., Ryzhik I.M. *Tablitsy integralov, summ, ryadov i proizvedeniy* (Tables of Integrals, Sums, Series, and Products) (Moscow: Nauka, 1971).
37. Lundskog J. *Scand. J. Plast. Reconstr. Surg*., **9**, 72 (1972).
38. Niemz M.H. *Laser-Tissue Interactions: Fundamentals and Applications* (Leipzig: Springer Science & Business Media, 2013).
39. Beacco C., Mordon S.R., Brunetaud J.M. *Proc. SPIE*, **1882**, 327 (1993).
40. Asimov M.M. *Opt. Spectrosc*., **115**, 774 (2013) [*Opt. Spektrosk*., **115**, 867 (2013)].
41. Chang C.J., Yu D.Y., Hsiao Y.C., Ho K.H. *Biomed. J*., **40**, 106 (2017).
42. Knyaz'kov V.B., Gofman V.V., Gofman V.R. *Lazernaya khirurgiya zabolevaniy glotochnogo limfaticheskogo kol'tsa* (Laser Surgery of Pharyngeal Lymphoid Ring Diseases) (Moscow: Tekhnosfera, 2016).
43. Elanchezhiyan S. et al. *Lasers Med. Sci.*, **28**, 7 (2013).
44. Parker S.P.A. *Laser-Tissue Interaction. In Lasers in Dentistry–Current Concepts* (Cham: Springer, 2017).
45. Bagratashvili V.I., Sobol E.N., Shekhter A.B. (Eds) *Lazernaya inzheneriya khryashchey* (Laser Engineering of Cartilages) (Moscow: Fizmatlit, 2006).
46. Forrer M., Frenz M., Romano V., et al. *Appl. Phys. B*, **56**, 104 (1993).